

Tuning the work function in transition metal oxides and their heterostructures

Z. Zhong¹ and P. Hansmann¹

¹Max-Planck-Institut für Festkörperforschung, Heisenbergstrasse 1, 70569 Stuttgart, Germany

(Dated: November 12, 2018)

The development of novel functional materials in experimental labs combined with computer-based compound simulation brings the vision of materials design on a microscopic scale continuously closer to reality. For many applications interface and surface phenomena rather than bulk properties are key. One of the most fundamental qualities of a material-vacuum interface is the energy required to transfer an electron across this boundary, i.e. the work function. It is a crucial parameter for numerous applications, including organic electronics, field electron emitters, and thermionic energy converters. Being generally very resistant to degradation at high temperatures, transition metal oxides present a promising materials class for such devices. We have performed a systematic study for perovskite oxides that provides reference values and, equally important, reports on materials trends and the *tunability* of work functions. Our results identify and classify dependencies of the work function on several parameters including specific surface termination, surface reconstructions, oxygen vacancies, and heterostructuring.

PACS numbers: 71.15.Mb

I. INTRODUCTION

One of the main goals of computational solid state physics is the simulation of “hypothetical” compounds that have not been synthesized in the experimental lab. Driven by its remarkable predictive power, Density functional theory (DFT) is today the most important tool in the field. Together with the high level of sophistication that synthesis technology has reached, the vision of materials design (i.e. the composition of functional materials that are tuned for usage in specific devices) seems to become reality. Control on the atomic level in materials synthesis e.g. with modern molecular beam epitaxy and pulsed laser deposition lead to an increasing focus on heterogeneous superstructures and effects associated with interfaces and surfaces. Especially oxide superstructures^{1,2} attracted lots of attention due to partially extraordinary physics^{3,4} unknown in the bulk materials but also adatom lattices or graphene grown on functional substrates are in the focus of current experimental and theoretical studies.

In our DFT study we concentrate on a particular quality of functional materials which is largely affected by its surface and crucial to many applications: the work function Φ . Devices that make use of thermionic electron emission⁵, catalytic surface properties⁶, construction of Schottky barriers⁷⁻⁹, or the conception of organic electronics^{10,11} are some of the technologies for which knowledge of the work function is essential. One of the main motivations for our study can be attributed to the very recent conception of so called thermoelectronic devices¹² which rely on the thermionic emission of an emitter and the subsequent condensation on a collector material. Being, so to speak, the next evolutionary step following thermionic energy converters, the new devices strive for a breakthrough in thermal to electrical energy conversion. Two main aspects are key for the novel setups: i) stability towards surface degradation also at

elevated temperatures and ii) emitter and collector materials with work functions tuned to one another. Due to these two criteria we focus our study on transition metal oxide (TMO) materials: Most TMOs are thermally very stable and have high melting points. Moreover, we know from an extensive body of research that TMOs are sensitive to external perturbations (i.e. they are *tunable*) which lead to rich phase diagrams¹³.

If we turn to past studies of density functional theory on materials work functions we find a good amount of research for simple metals¹⁴⁻¹⁶, molecular structures^{17,18} and simple oxides like MgO and ZnO^{19,20} on metal surfaces, Sc₂O₃ with adsorbed Ba²¹, modified silicon (111) surfaces²², and even graphene^{23,24}. Yet, TMO work functions have been rarely studied and only recently started to attract attention^{25,26}.

In the present study we clarify the sensitivity of TMO work functions with respect to the specific surface termination, surface relaxation, surface reconstruction, defect structures (i.e. oxygen vacancies), externally induced surface strain, electronic interactions on the mean-field level (i.e. inclusion of a Hubbard U), and most importantly, material trends for a number of perovskite oxides and superstructures. Our findings will not only serve as a reference for the presented compounds but especially the observed parameter trends present a first systematic step towards a broader understanding of how to push a compounds work function to the desired value.

The manuscript is organized in the following way: After reporting details of our calculation scheme in section II we divide our results in three sections. In section III we report on the sensitivity of the work function on “external” and calculation parameters. While some of the calculation parameters serve purely as a DFT benchmark (e.g. choice of the DFT functional or the Hubbard interaction U), others will be quite relevant for comparison to experimental dependencies (e.g. lattice strain or oxygen vacancies). In section IV we explore the material trends

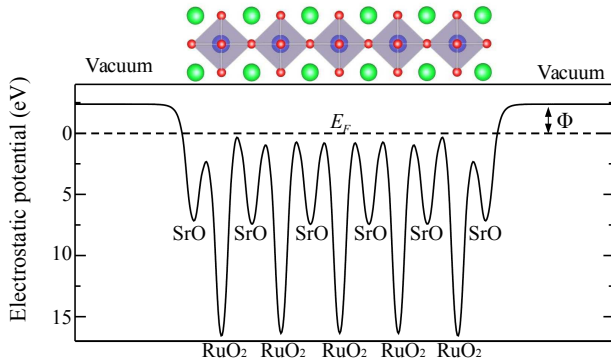


FIG. 1: Plane averaged electrostatic potential of a symmetric SrRuO_3 slab consisting of six SrO layers, five RuO_2 layers, and a 20 Å vacuum. The electrostatic potential is defined with respect to Fermi energy E_F , and converges to a constant value in the vacuum region that is the work function Φ of SrRuO_3 with SrO surface termination. Φ therefore indicates the required energy to remove an electron at Fermi level from the material to a state at rest in the vacuum nearby the surface.

for different ABO_3 perovskite oxides. In section V we consider the potential of tuning work functions with heterostructuring oxide materials.

II. BACKGROUND AND CALCULATION DETAILS

The work function is defined as the minimal energy required to remove an electron from inside the material across its surface into the vacuum. Conceptually the work function can be divided into a “bulk” and “surface” dependent part. If there were no charge redistribution at a materials surface and the vacuum potential would be set to $V_{\text{vac.}} = 0$, the work function would be equivalent to $\Phi = V_{\text{vac.}} - E_F$ (where E_F is the materials Fermi energy). (see e.g. Ref. 27). In reality, however, ionic and electronic charge in the vicinity to the surface is very different from the bulk and an additional electric field is generated by the non vanishing dipole moment of the shifted charge arrangement. It is intuitively clear that generally such a field, and therefore also the work function, depends on the specific surface indices and termination. For our studies we assume clean surfaces with well defined terminations. Let us remark already here that while there are many materials, in particular simple metals²⁸, which show little dependence of the work function on microscopic details of the surface, TMO work functions are extremely sensitive to these details.

In this study we have selected a number of perovskite transition metal oxides ABO_3 (where $A=\text{Ca, Sr, Ba}$;

$B=3d, \text{Ti-Co}; 4d: \text{Zr-Rh}$) and their heterostructures. The ABO_3 structure can be viewed as simple cubic lattice of A atoms with a body centered B atom and oxygen atoms in the face centers. In the following we consider surfaces along the (001) direction which are the most commonly studied surfaces in thin film or heterostructure compounds. In this direction the crystal is built up by an alternating stacking of AO and BO_2 layers³. The (001) ABO_3 then have either AO or BO_2 surface terminations, and thus two intrinsically different work functions. For the calculation of the work function within a DFT framework we employ a symmetric slab geometry which is sketched in the top part of Fig. 1 for the example of SrRuO_3 . The SrO terminated SrRuO_3 slab consists of six SrO layers, five RuO_2 layers, and a vacuum thickness of 20 Å; for BO_2 terminated surface (not shown in Fig. 1) we add an additional BO_2 layer on each side of the slab. The work function Φ is then calculated as the energy difference between the plane averaged electrostatic potential (excluding the exchange correlation part) of the slab in the vacuum region and the Fermi level as can be seen in Fig. 1; Benchmark calculations confirmed that Φ is converged with this setup. For further information on the calculation of the averaged electrostatic potential we refer to 23 and 17.

Since we are mostly interested in materials and superstructures grown on substrates, the in-plane lattice constant was fixed to $a=3.905\text{Å}$ which is that of an assumed undistorted cubic SrTiO_3 substrate (it is also very close to the bulk lattice constant $a=3.923\text{Å}$ of cubic SrRuO_3 ²⁹). For all calculations the internal atomic positions were relaxed. The calculations were performed with the VASP (Vienna ab initio simulation package) code³⁰ using the generalized gradient approximation GGA -PBE functional³¹ for electronic exchange and correlation and a $16\times 16\times 1$ k-point grid including the Γ point. In a set of selected benchmark calculations we compare the GGA results also to those obtained by a local-density approximation (LDA) functional³². While the latter one generally leads to somewhat larger values of the work function, our main conclusions about materials trends and sensitivities remain unchanged by the choice of the functional. Let us also explicitly mention that this study is not concerned with the temperature dependence of the work functions. While motivated by applications and devices which operate at elevated temperatures the non-trivial inclusion of finite temperatures in DFT calculations is beyond the scope of this study.

III. RESULTS A: EXTERNAL PARAMETERS

Part of our first set of calculations in which we identify key parameters that alter the work function can be considered as DFT benchmarks. Obviously, if the parameter in question is experimentally accessible (like e.g. substrate strain), one can deduce potential tuning parameters of Φ .

TABLE I: Work function of SrRuO₃ and SrTiO₃ with either SrO or (Ru,Ti)O₂ surface terminations. The table summarizes dependencies of the work function for i) different choices of the DFT functional (columns 3 & 4), ii) an unrelaxed lattice (column 5), iii) compressive (a=3.80Å) or tensile (a=4.00 Å) strained substrate (columns 6 & 7), iv) ferromagnetic ground state of SrRuO₃ with an on-site Coulomb repulsion U=2.0eV (column 8), v) a monolayer film; the low temperature orthorhombic structure of SrRuO₃; SrTiO₃ with a TiO₂ 2×1 surface reconstruction (columns 9,10,11), vi) with surface oxygen vacancies in top layer/subsurface layer (column 12), vii) values observed in experiment

Φ in eV	term.	LDA	GGA	unrelaxed	a=3.80	a=4.00	U=2eV	monolayer	orthorhombic	reconstruct	Ov	exp
SrRuO ₃	SrO	2.80	2.39	1.30	2.00	2.55	2.37	2.60	2.29	-	2.05/2.39	5.2 ^a
	RuO ₂	5.01	4.88	3.90	5.54	4.92	5.33	4.95	5.05	-	5.03/4.91	
SrTiO ₃	SrO	2.52	1.92	0.82	1.69	2.04	-	2.02	-	-	2.26/1.33	2.4 ^b
	TiO ₂	4.67	4.48	3.70	4.47	4.51	-	4.18	-	6.18	3.39/3.86	4.6 ^b

^aFang *et al.* Ref. 33 with unknown surface termination

^bSusaki *et al.* Ref. 34

The results we report in this section are obtained for SrRuO₃ and SrTiO₃. Both materials are well studied and experimental data for their work functions are available^{33,34}. SrRuO₃ is a *4d* system and a ferromagnetic metal³⁵; SrTiO₃ on the other hand is a *3d* non-magnetic insulator. At this point we should make some more specific remarks about how we deal with the calculation of work functions for the insulating SrTiO₃. The difficulty for insulators is the uncertainty of the Fermi energy which needs to be subtracted from the vacuum potential to yield Φ . Instead, we decided to consider the bottom of the conduction band as the Fermi energy due to a simple and pragmatic argument: Our choice corresponds to the electron doped version of the material which can be realized in experiment by La substituting Sr³⁶, or by Nb substituting Ti. The later technique was used in a work function study for SrTiO₃ by Susaki *et al.*³⁴ and as one can see in Fig.1 thei calculated values based on our definitions are in satisfactory agreement with the experimental observations. Moreover, even without active doping, the (very common) occurrence of oxygen vacancies in TMO surfaces effectively lead to the same kind of doped electronic structure. Let us anticipate already here that our calculations, which include such oxygen vacancies explicitly, do not capture effects from an insulator to metal transition but rather from very small to very large concentration of oxygen vacancies. For these cases of slightly doped insulators, where the work function might rely sensitively on the size of the gap between conduction and valence band, we also make sure that DFT-GGA, which is known to underestimate gap sizes and the Heyd-Scuseria-Ernzerhof (HSE) hybrid functionals^{37,38} (known to yield better results for band gaps) yield consistent results for Φ . We summarize our parameter study in Table I. Here, we report values for both materials and consider either a SrO terminated or a (Ru,Ti)O₂ terminated (001) surface.

The values of Φ in the first column of Table I obtained with plain GGA for relaxed slabs already show an extremely important effect that we observe in basically all calculations we have performed: Different from simple metals like tungsten or silver, where the work function

shows a surface dependence on the order of hundreds of meV²⁸, the work function for perovskite oxides shows a much more severe modulation with the choice of a specific surface, e.g. if it is AO or BO₂ terminated. From our calculations we observe a difference of $\Phi_{\text{BO}_2} - \Phi_{\text{AO}} = 2.49\text{eV}$ (2.56eV) for SrRuO₃ (SrTiO₃) which prohibits clearly an approximation of Φ by a single Φ_{ABO_3} value for oxide materials and sets the challenge for a theory/experiment comparison: control of the sample on sub-unit cell scale seems necessary in synthesis to support/falsify predictions from computer simulations. If such control is not possible, the samples might have mixed termination and, hence, display a strong sensitivity of the work function to details of the sample preparation. Such difficulties might be one of the reasons that as of yet there are only few experimental studies on TMO work functions^{33,34,39}. Moreover, these complications also affect the conception of interface devices like, e.g., TMO Schottky barriers at metal/semiconductor interface where the barrier height is calculated with the work function of the metal⁷. We will return to the discussion of termination dependent work function in the context of building up superstructures (see section V).

Let us turn to the comparison of GGA with LDA results. Our test cases are actually well in line with an extensive study of Singh-Miller and Marzari¹⁶, where the functional dependence of DFT workfunctions for metallic surfaces is discussed. The differences between GGA and LDA can be attributed on the one hand to differences in the relaxed structure (since GGA, e.g. generally overestimates bondlengths when compared to experiment). On the other hand, when performed for identical lattices LDA tends to yield always somewhat larger values than GGA. As can be seen in Table I we observe total differences between $\approx 0.13 - 0.50\text{eV}$. While these differences are surely non negligible and one should be aware of possible error bars. Relative values and materials trends, however, are not affected.

More crucial than the choice of the particular DFT functional is, however, the relaxation of the atomic positions in the unit cell near the surface with respect to an unrelaxed surface. Work functions calculated with un-

relaxed surfaces differ partially more than 1.0eV from the relaxed calculations. In our calculations the surface relaxation always increases the work function which means that the surface dipole-field increases. It is tempting to attribute this increase just to a surface buckling that features an outward shift of oxygen ions at the surface (stronger for AO than for BO_2 terminated surfaces). On quantitative levels a purely ionic picture is, however, misleading since it disregards effects of relaxation of the electronic charge involving interlayer charge transfer. The sensitivity that we observe here indicates already the strong dependence of the work function on microscopic details of the surface as can be seen also in the calculations for either compressive ($a = 3.80\text{\AA}$) or tensile ($a = 4.00\text{\AA}$) strain which can be achieved with growing the material on specifically chosen substrates. It turns out that in this way modification of the work function can be achieved over a range of up to $\approx 0.7\text{eV}$. In the SrO terminated compounds we always find a decrease (increase) of the work function upon compressive (tensile) strain. In the BO_2 terminated compounds we see a clear difference between the metallic RuO_2 layer which shows an increase of the work function upon either compressive or tensile strain, while the TiO_2 terminated systems is affected by the pressure only on a very small scale compared to the other cases.

Next we turn to the question whether a Hubbard U interaction parameter on the B atom d-shell treated on the mean-field level has impact on Φ . Such additional local potential will only have impact in cases of partially filled shells which is why an interaction $U = 2.0\text{eV}$ was taken into account only for the ruthenate calculation. We have carried out the GGA+ U calculation⁴⁰ where we allowed for a ferromagnetic symmetry broken ground state. It does not come as a big surprise that the RuO_2 terminated surface is more influenced by the U on the Ru d-shell which results in a work function enhancement by $\approx 0.4\text{eV}$ while the AO terminated surface is basically unaffected. For the general case, however, please note that electronic interaction/correlation (approximated on the Hartree level or beyond) might trigger phase transitions that result in a charge redistribution, e.g. surface charge-ordered states⁴¹ which might have significant impact on the surface dipole field and, hence, its work function. Let us briefly point out that we did not consider a GGA+ U calculation for the band-insulating SrTiO_3 with a practically empty d-shell. U would simply enlarge the gap by pushing up empty states. Since not much is gained by such a manual gap renormalization we state that the most reasonable step would rather be a GW calculations without adjustable parameters which, however, is beyond the scope of our current study.

The following three calculations consider again more structural effects: In monolayer setups effects of quantum confinement can alter the electronic structure^{42,43}. Also we remark that for most ABO_3 materials, the low temperature structure is not cubic but often shows orthorhombic distortions with tilted and rotated BO_6 oc-

tahedron, which, however, do not alter Φ dramatically. Moreover, we argue that simulations for Φ should rather consider the materials structure at the operation temperature of the hypothetical device. Also, depending on the temperature, we take into account that for real oxide surfaces, various surface reconstructions exist (for example of SrTiO_3 ⁴⁴⁻⁴⁷). It is reasonable to assume that the different structure of bonds and hence electronic densities in reconstructed surfaces will lead to specific dipole fields and, hence, altered work functions. We confirmed this hypothesis by studying a well-established so called (2×1) surface reconstructed phase of SrTiO_3 ⁴⁶, which can be viewed as a double TiO_2 layer. It turns out that the reconstruction has a great influence on the work function which is, with a value of 6.18eV, much higher than the 4.48eV of the bare TiO_2 surface.

Finally, it is a well known issue for oxide surfaces that defects in the form of oxygen vacancies should not be disregarded^{48,49}. While there is a certain amount of control over oxygen vacancies in synthesis (e.g. adjusting the oxygen pressure and annealing) the exact concentration and distribution is generally unknown and hard to pin down. Such defects pose a real challenge to comparing different experiments, but also experiment to an electronic structure calculation of the oxide surfaces. The best one can do in a calculation is to assume periodic vacancies in supercells. In our case we assume a 2×2 supercell and introduce for each case considered an oxygen vacancy in the surface or the first subsurface layer. With this setup we actually assume a quite high concentration of oxygen vacancies so that our results for Φ might be considered as an upper bound of the O vacancy effect.

As conclusion of this section stands a classification of external parameters by means of their impact on a materials work function. The first and most important message is that for transition metal oxide work functions the microscopic structure of the surface electronic states/density *does* matter crucially. While our analysis underlines the challenging (but nowadays feasible) necessity of experimental control on the atomic scale it also tells us that a materials *work function can be tuned* with a number of external parameters. While magnetism (in the tested cases), interaction effects or even “quantum confinement” effects are not major (Φ converges rather quickly as a function of thickness), clean terminations and control of surface reconstructions is absolutely mandatory. The latter parameters can tune the work function on the scale of electron volts. On a smaller scale ($\approx 0.5\text{eV}$) the work function can be modified, i.e. fine tuned, by exerting control on the oxygen defect structure and/or the choice of substrate. With these results in mind we will now turn to another type of “control parameter”: The choice of alkali earth cation A cation and transition metal element B.

IV. RESULTS B: ABO₃ MATERIAL TRENDS

As mentioned before the results in this section were obtained from setups with a fixed in-plane lattice constant of $a=3.905\text{\AA}$ which corresponds to growth on a SrTiO₃ substrate. To disentangle trends originating in the specific choice of cation (A) and TM (B) from other parameters (see previous section) we consider defect free, relaxed structures with well defined terminations in a GGA slab calculation. The results are reported in Fig. 2 and 3 (and corresponding data tables in appendix A).

A. Termination dependence in different materials

Overall we find as a first remarkable fact a confirmation of the crucial dependence of Φ on the termination, see Fig. 2 and 3. Except for a single case (CaZrO₃) the work function of the AO terminated surface is smaller than the BO₂ terminated one. It turns out that this observed materials dependence hints towards a new twist to the interpretation of the termination sensitivity: We remind ourselves that the surface dependence of the work function originates in the dipole field created by polarization of the electronic charge and shifts of atoms/ions close to the specific surface. Two effects which are obviously coupled in our calculations which include a self consistent lattice relaxation. While this interplay is quite involved and cannot be disentangled easily, we observe a clear correlation between the work function behavior and the *electronegativity* χ of the cation and transition metal elements⁵⁰.

The concept of electronegativity is usually used in order to estimate the character of an ionic bond in a binary compound. Taking the difference of the two elements electronegativity allows for classification of the bond into either ionic or covalent. So χ *reflects the ability of an atom to attract electron density*. Keeping this in mind it comes not as a big surprise that for simple metals the compounds work function is linked to the elements electronegativity⁵¹. Our results and analysis show that, remarkably we can still use the electronegativity concept in our ternary compounds. Following the Allen scheme⁵⁰ of electronegativity we find a monotonous increase in χ_B from Ti ($\chi_{\text{Ti}} = 1.38$) to Co ($\chi_{\text{Co}} = 1.84$) for the 3d series, a monotonous increase from Zr ($\chi_{\text{Zr}} = 1.32$) to Rh ($\chi_{\text{Rh}} = 1.56$) for the 4d series, and for the cations we have $\chi_{\text{Ca}} = 1.03$, $\chi_{\text{Sr}} = 0.96$, and $\chi_{\text{Ba}} = 0.881$ ⁵⁴ Oxides are typically considered as very ionic due to the high electronegativity of oxygen $\chi_{\text{O}} = 3.61$.

For our materials it turns out to be useful to introduce the idea of a layer electronegativity χ_{AO} and χ_{BO_2} . In all considered compounds χ of cation A is smaller than that of transition metal B so that on the one hand A-O bonds can be considered as more ionic than B-O bonds but also that the average AO electronegativity is smaller than that of the BO₂ layers $\chi_{\text{AO}} < \chi_{\text{BO}_2}$. This explains the general tendency of smaller AO work functions $\Phi_{\text{AO}} <$

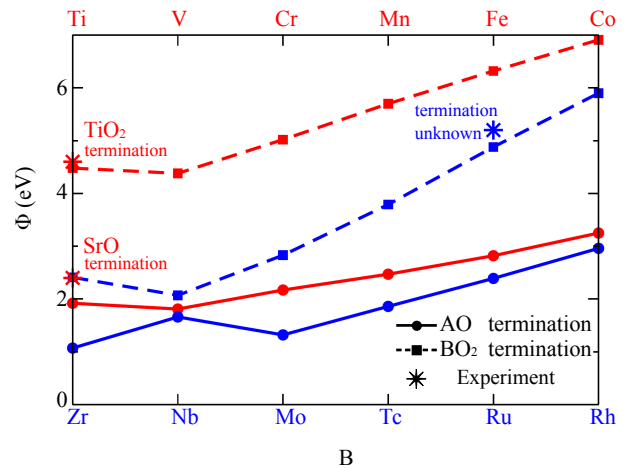


FIG. 2: DFT calculated work functions of the perovskite ABO₃ series with A=Sr and B being an element of the 3d (red) or 4d (blue) period, and with AO (circle with solid lines) and BO₂ (square with dashed lines) surface termination. Experimental work function of SrTiO₃ with SrO and TiO₂ termination by Susaki *et al.* 34 as well as SrRuO₃ with unknown termination by Fang *et al.* 33 are shown as stars.

Φ_{BO_2} which we already reported. It turns out that with these rough estimates many of the following materials trends can be explained.

B. Control via transition metal B for A=Sr

We will now discuss tuning of the work function with choice of the transition metal element B in more detail. As shown in Fig. 2 we have performed calculations for a series of 3d and 4d transition metal compounds. The overall variation of the work function is a remarkable 6eV ($\approx \Phi_{\text{SrCoO}_3}^{\text{BO}_2} - \Phi_{\text{SrZrO}_3}^{\text{AO}}$). Continuing the line of argument from above, the trends we observe can be explained by comparison of χ_B of the transition metal element (or the effective BO₂ electronegativity χ_{BO_2}). It is no surprise that the trend is weaker in the case of AO termination since increased χ_{BO_2} in the subsurface layer has less effect on Φ . The increasing Φ within each series (3d,4d) reflects precisely the increase of χ_{BO_2} within the period and so does the decrease of $\Phi_{3d} < \Phi_{4d}$ reflect $\chi_{3d} < \chi_{4d}$. A closer look at the numbers shows indeed quite low work functions for AO termination throughout the series and an almost monotonous increase from $\Phi_{\text{SrTiO}_3} \approx 1.9\text{eV}$ (3d series) and $\Phi_{\text{SrZrO}_3} \approx 1.1\text{eV}$ (4d series)⁵⁵ to $\Phi_{\text{SrCoO}_3} \approx 3.2\text{eV}$ and $\Phi_{\text{SrRhO}_3} \approx 3.0\text{eV}$ with the only exception of Φ_{SrNbO_3} being slightly higher than Φ_{SrMoO_3} . We find the same trend in the BO₂ terminated surfaces of these materials though at values for Φ which are roughly larger by a factor of 2.

Before we continue our discussion for cation controlled tuning of Φ let us compare the results to the few ex-

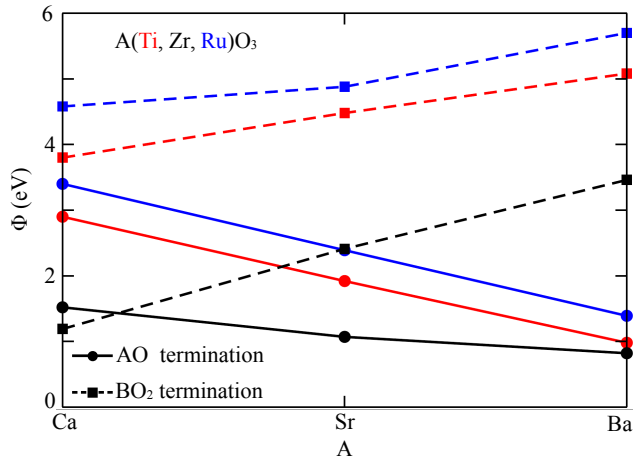


FIG. 3: DFT calculated work functions of the ATiO_3 (red), AZrO_3 (black), and ARuO_3 (blue) series with $\text{A}=\text{Ca}$, Sr and Ba , and with AO (circle with solid lines) and BO_2 (square with dashed lines) surface termination.

perimentally available data points (shown as “stars” in Fig. 2). For SrTiO_3 both values for TiO_2 or SrO terminated surfaces³⁴ are in very satisfactory agreement with our calculations. (The comparison shows further that due to the very likely presence of oxygen vacancies it is a reasonable ansatz to take the energy of the lowest (electron doped) conduction band as reference energy for Φ). The only other data point is that of SrRuO_3 for which, however, the precise termination was undetermined³³. In fact one is tempted to conclude by comparison to our results that the termination was most likely a RuO_2 dominated one. Yet, one has to be careful since rough surfaces are most probably determined not only by a mixture of AO and BO_2 domains but also by polarizability of defects like domain walls etc.. We use this observation to emphasize once more the importance of microscopic control of the surface structure if comparison or predictions of calculations like ours should be considered. Moreover, if oxide heterostructures are used in devices like Schottky barriers⁷⁻⁹ or for organic electronics^{10,11} the oxide work function is often used as for simple metals or semiconductors. We emphasize once more, however, that this is very dangerous since *there is no such thing as a single valued work function for an oxide material*.

C. Control via cation A

We now turn to control of the work function with the choice of the alkaline earth cation A. In Fig. 3 we report results obtained for nine selected compounds $(\text{Ca}, \text{Sr}, \text{Ba})(\text{Ti}, \text{Zr}, \text{Ru})\text{O}_3$ to study trends with the cation choice. As a first observation we state that the overall dependence of Φ is quite large and that the cation choice is apparently a promising tuning parameter. The

changes in the AO terminated surfaces are more sizable than before and follow the trend of electronegativity of the cation: Ba has the smallest χ , and hence the smallest work functions. However, the trend in BO_2 terminated surfaces with cation A is not as easily explained! While χ_A decreases from Ca to Ba , the work function for BO_2 terminations actually increases. This points towards an aspect which is not taken into account by our simple electronegativity argument: *Charge transfer* between AO and BO_2 layers. One possible explanation is that more ionic AO layers lead to an increased charge transfer to the terminating BO_2 layer which then increases the dipole field and, hence, the work function. On the other hand we cannot underline this hypothesis with evidence and remain with reporting the observed trend.

D. Promising materials

At the end of our materials study we can confirm experimental strategies with our calculations that have been established on an empirical basis in the past. The electronegativities χ_A and χ_B might be used (keeping the limitations of the estimate in mind) as a rough guidance to select promising materials. Our considered materials cover a wide range of work functions reaching from 6.91eV (CoO_2 terminated SrCoO_3) down to 0.82eV (BaO terminated BaZrO_3). For electron emitting devices and, more specifically, emitter and collector materials in thermoelectronic setups one needs low work functions. These are found in the compounds of the early elements in the $3d$ and $4d$ series: First of all we point out SrO terminated SrMoO_3 ($\Phi_{\text{SrMoO}_3}^{\text{SrO}}$) which is the material with the highest conductivity in our $4d$ series. It can be grown in thin films by pulsed laser deposition⁵² and would be a good candidate, e.g. for the electrode material in thermoelectronic devices. Another very interesting compound we would like to highlight is CaZrO_3 . It is remarkable due to the fact that the work function is at the same time quite low *and* rather similar for both terminations (see Fig.3). This means, that also less clean (heterogeneous) CaZrO_3 (001) surfaces, which are much less tedious/expensive to synthesize, will be good electrode materials. Third, our results for BaBO_3 are in agreement with the well known observation that coverage with BaO will lower a materials work function *if AO terminated systems are concerned*. This last conclusion leads us to our third and last section where we discuss how to tune the work function by building heterostructures.

V. RESULTS C: OXIDE HETEROSTRUCTURES

In the previous section we have already made several observations how (and gave arguments why) changes in surface layer and charge transfer between layers close to the surface affect the work function. In the third and final part of our study we turn to even more drastic sur-

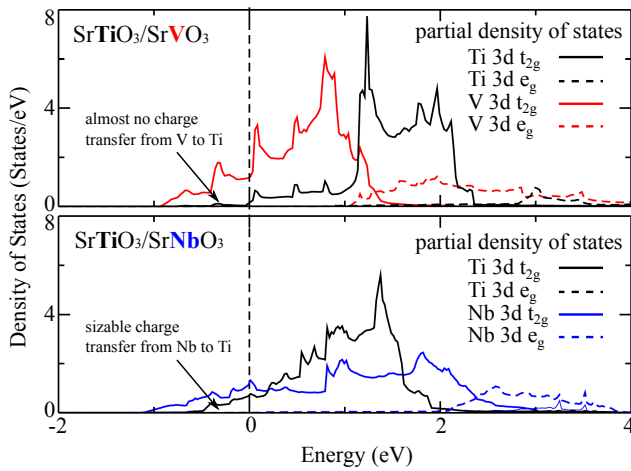


FIG. 4: DFT calculated density of states for SrVO₃ capped with one unit cell of SrTiO₃ (upper panel) and SrNbO₃ capped with one unit cell of SrTiO₃ (lower panel). We show only the partial density of states for V, Nb, and Ti 3d-states. t_{2g} and e_g states are indicated by solid and dashed lines respectively. The figure shows a clear material dependence of the charge transfer between base and capping material.

face manipulation: instead of just choosing one of the materials lattice planes to be the surface layer we build the surface actively by combining different compounds.

To this end we model symmetric A'B'O₃/ABO₃ heterostructures by adding A'B'O₃ thin films (grown in the 001 direction) with varying number of unit cells N on both sides of the ABO₃ slab (i.e. capping) with either AO or BO₂ termination. To be more specific, an AO terminated material capped with A'B'O₃ will have an A'O interface with vacuum while a BO₂ terminated one will have a B'O₂ interface with vacuum.

TABLE II: Work function of SrVO₃, SrNbO₃ and SrRuO₃ capped by SrTiO₃ thin films. The thickness of SrTiO₃ N is varied from 0 to 2

SrTiO ₃	SrVO ₃		SrNbO ₃		SrRuO ₃	
	SrO	VO ₂	SrO	NbO ₂	SrO	RuO ₂
$N=0$	1.81	4.38	1.66	2.07	2.39	4.88
$N=1$	1.88	4.61	1.18	3.41	2.17	4.72
$N=2$	1.87	4.77	1.29	3.82	2.13	4.87

A. Non-polar capping:

In table II we present results for capping three example materials with SrTiO₃ of varying thickness of either one or two unit cells (as well as the reference $N=0$ for the uncapped material). SrTiO₃ is a charge neutral and non-polar band insulator. The results depend strongly on the specific case. The most severe change is found

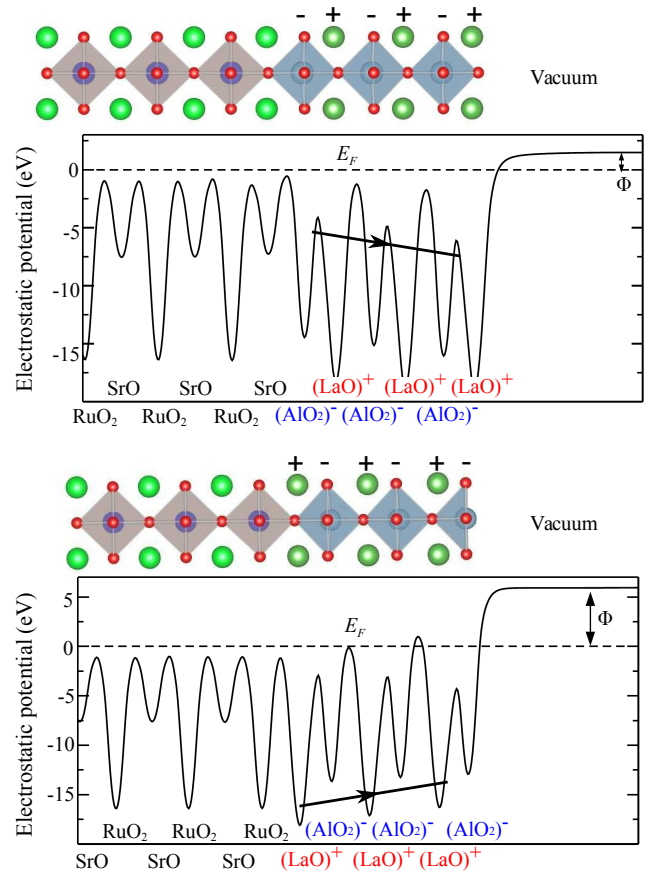


FIG. 5: Plane averaged electrostatic potential for a LaAlO₃/SrRuO₃ heterostructure calculated with DFT: three layers of LaAlO₃ grown on a SrRuO₃ substrate with AO termination (upper panel) or BO₂ termination (lower panel). The internal field of the polar layers tunes the work function depending on its direction.

in SrNbO₃ capped with one unit cell of SrTiO₃. Here the work function is reduced for the SrO termination from 1.66eV to 1.18eV while the NbO₂ terminated (i.e. TiO₂ as final layer) compound experiences an increase of the work function from 2.07eV to 3.41eV. By comparison changes in SrVO₃ or SrRuO₃ are less pronounced. The reason for this different behavior is found when we study the charge transfer between base and capping material. In Fig. 4 we show the partial density of states for SrTiO₃/SrVO₃ (upper panel) and SrTiO₃/SrNbO₃ (lower panel).

The local potential of Ti d orbitals in SrTiO₃ turns out to be comparable to the Nb d potential in SrNbO₃. V d orbitals in SrVO₃, however, reside at a much lower energy⁵³. As a consequence we encounter a substantial charge transfer in SrTiO₃/SrNbO₃ (as seen in Fig.4), while basically no charge transfer occurs in SrTiO₃/SrVO₃. As one can from the lower panel the Ti d-states in the SrTiO₃/SrNbO₃ system are heavily electron doped by the base material while this is not the

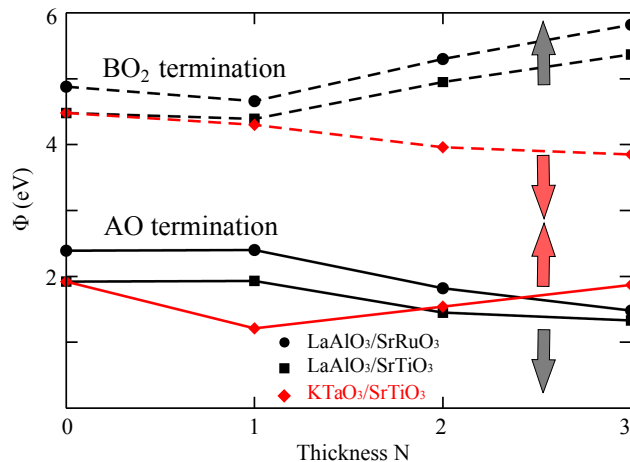


FIG. 6: Work function plotted versus thickness of polar capping material. As already indicated in Fig. 5 the additional field produced by polar layers can be used to tune the work function in either way. Here we show how either termination can be tuned up or down by choosing the appropriate capping material LaAlO_3 or KTaO_3 which have opposite effects due to their opposite polarity.

case for the vanadate case. Such doping has severe consequences not only by shifting the Fermi level into the Ti d-states but also by actually charging the capping layer which alters the surface dipole field. It is interesting how such complex interplay of lattice, orbital and charge degrees of freedom eventually leads to a work function for the AO terminated surface which is lower than that of the parent compounds SrTiO_3 or SrNbO_3 . This case confirms, as a proof of principle, the potential of tuning Φ by heterostructuring oxide materials.

One should remark that in the example we have just discussed the capping material was an insulator. If we choose $\text{A}'\text{B}'\text{O}_3$ to be a metal, we see that the work function is dominated by the $\text{A}'\text{B}'\text{O}_3$ thin films (so that the capped ABO_3 material is almost entirely irrelevant). This is simply due to the screening properties of the metallic capping compound and we could only study the strain and quantum confinement effect in $\text{A}'\text{B}'\text{O}_3$.

B. Inducing intrinsic fields by polar capping

When $\text{A}'\text{B}'\text{O}_3$ is a polar insulator, such as LaAlO_3 , which can be viewed as an alternating stack of positively charged $(\text{LaO})^+$ layers and negatively charged AlO_2^- layers. When it is grown on a non-polar compound like SrRuO_3 or SrTiO_3 (charge neutral $(\text{SrO})^0$ and $(\text{Ru,Ti})\text{O}_2^0$ layers), A possible hypothesis that was studied in the past³⁴ is that thin films of a polar material (e.g. LaAlO_3) play the role of a parallel capacitor that introduces an internal electric field pointing from surface, e.g. LaO , layer to the interface of e.g. SrO/AlO_2 . The resulting

potential drop should lead, as the polar capping material thickness increases, to a decrease of the work function. We sketch this scenario in Fig. 5: the result for LaAlO_3 (KTaO_3) capping would be a decrease (increase) of the work function for the AO and an increase (decrease) for the BO_2 terminated case. We performed calculations for SrRuO_3 or SrTiO_3 for LaAlO_3 and KTaO_3 capping of different thickness and present the results in Fig. 6. Let us first remark that the comparison between $N=0$ and $N=1$ is always delicate since we introduce not only the additional field but also the surface relaxation changes most from the uncapped to the $N=1$ case. The data from $N=1$ to $N=3$ shows that the DFT calculation confirms the simple hypothesis for all checked cases: LAO capped AO surface layers show decreasing Φ with increasing N while LAO capped BO_2 terminated cases show an increase. The opposite is true for capping with KTaO_3 . In principle this observation is encouraging. However, these observations are in contradiction to experiments performed by Susaki et al.³⁴. In their article the authors already mention the discrepancy of the simple “additional internal field” picture with their measured data: Instead of a work function increase they found a remarkable decrease in TiO_2 terminated SrTiO_3 capped with LaAlO_3 .

In summary we report that DFT results agree with the simple picture of superimposed potentials but not with experiment. A reasonable explanation for the discrepancy might be found in defect structures not taken into account by our calculations. In section III we have seen that oxygen vacancies can alter the work function on a significant scale so that a disregard of likely defects in the LaAlO_3 capped systems is not justified.

VI. CONCLUSION:

In conclusion we have presented a systematic work function study for transition metal compounds which allowed us to classify the sensitivity of the work function to parameters of DFT calculations as well as to experimentally accessible conditions like oxygen vacancies, substrate strain, and heterostructuring. We were able to conclude, on general grounds, that the work function concept is more complex in oxide materials than in simple metals and that microscopic details at the materials surface matter crucially. We emphasize that tuning oxide work functions (predictably) in the experimental lab generally requires synthesis control on the atomic scale. This challenge comes, however, with the prize that oxide work functions are indeed highly tunable and, depending on the parameter can be manipulated on different energy scales. While the choice of the material and the choice of the terminating layer tunes oxide work functions over several eV, substrate induced strain or a suitable capping material can fine tune the work function on the sub-eV scale to the desired value. We have also uncovered that, like for simple metals, there is a link between the observed

work function Φ and electronegativities χ_A and χ_B of the elements in the compound which was helpful in explaining the observed materials trends and might prove to be also useful for extrapolating our results in other directions. For the manipulations of Φ with polar capping layers we conclude from our theory/experiment comparison with a warning that for real materials an oversimplified electrostatic picture is highly doubtful.

Let us finally remark that one of the main intentions of this manuscript is to form a fix point for future studies. The “phase space” of materials and tuning parameters is infinitely large so that any systematic search needs a well established base. We hope that also experimental colleagues can help to judge the quality of the many data points we predicted for materials that have not yet been measured in order to establish such a base.

VII. ACKNOWLEDGMENTS

We thank J. Mannhart, I. Rastegar, G. Giovannetti, N. Spaldin, and L. Giordano for motivation and useful discussions.

Appendix A: Φ Tables

TABLE III: Data of Fig. 2: Work functions of SrBO_3 (B=3d, Ti-Co; 4d: Zr-Rh) with SrO and BO_2 surface terminations

3d SrBO_3	Ti	V	Cr	Mn	Fe	Co
AO	1.92	1.81	2.17	2.47	2.82	3.25
BO_2	4.48	4.38	5.02	5.70	6.32	6.91
4d SrBO_3	Zr	Nb	Mo	Tc	Ru	Rh
AO	1.07	1.66	1.32	1.86	2.39	2.96
BO_2	2.41	2.07	2.83	3.79	4.88	5.90

TABLE IV: Data of Fig. 3: Work functions of ABO_3 (A=Ca, Sr, Ba; B=Ti, Zr, Ru) with AO and BO_2 surface terminations

	ATiO_3		AZrO_3		ARuO_3	
	AO	TiO_2	AO	ZrO_2	AO	RuO_2
A=Ca	2.90	3.80	1.52	1.19	3.40	4.58
A=Sr	1.92	4.48	1.07	2.41	2.39	4.88
A=Ba	0.98	5.08	0.82	3.46	1.39	5.70

-
- ¹ J. Mannhart and D. G. Schlom, *Science* **327**, 1607 (2010).
- ² P. Zubko, S. Gariglio, M. Gabay, P. Ghosez, and J.-M. Triscone, *Annual Review of Condensed Matter Physics* **2**, 141 (2011).
- ³ A. Ohtomo and H. Y. Hwang, *Nature* **427**, 423 (2004).
- ⁴ N. Reyren, S. Thiel, A. D. Caviglia, L. F. Kourkoutis, G. Hammerl, C. Richter, C. W. Schneider, T. Kopp, A.-S. Rüetschi, D. Jaccard, et al., *Science* **317**, 1196 (2007).
- ⁵ S. Yamamoto, *Reports on Progress in Physics* **69**, 181 (2006).
- ⁶ J. Suntivich, H. A. Gasteiger, N. Yabuuchi, H. Nakanishi, J. B. Goodenough, and Y. Shao-Horn, *Nature Chemistry* **3**, 546 (2011).
- ⁷ Y. Hikita, Y. Kozuka, T. Susaki, H. Takagi, and H. Y. Hwang, *Applied Physics Letters* **90**, 143507 (2007).
- ⁸ M. Minohara, R. Yasuhara, H. Kumigashira, and M. Oshima, *Phys. Rev. B* **81**, 235322 (2010).
- ⁹ T. Yajima, Y. Hikita, M. Minohara, C. Bell, J. A. Mundy, L. F. Kourkoutis, D. A. Muller, H. Kumigashira, M. Oshima, and H. Y. Hwang, *Nat. Comm.* **6**, 6759 (2015).
- ¹⁰ M. T. Greiner, M. G. Helander, W.-M. Tang, Z.-B. Wang, J. Qiu, and Z.-H. Lu, *Nat. Mat.* **11**, 76 (2012).
- ¹¹ M. T. Greiner and Z.-H. Lu, *NPG Asia Materials* **5**, e55 (2013).
- ¹² S. Meir, C. Stephanos, T. H. Geballe, and J. Mannhart, *Journal of Renewable and Sustainable Energy* **5**, 043127 (2013).
- ¹³ M. Imada, A. Fujimori, and Y. Tokura, *Rev. Mod. Phys.* **70**, 1039 (1998).
- ¹⁴ H. L. Skriver and N. M. Rosengaard, *Phys. Rev. B* **46**, 7157 (1992).
- ¹⁵ M. Methfessel, D. Hennig, and M. Scheffler, *Phys. Rev. B* **46**, 4816 (1992).
- ¹⁶ N. E. Singh-Miller and N. Marzari, *Phys. Rev. B* **80**, 235407 (2009).
- ¹⁷ P. C. Rusu and G. Brocks, *Phys. Rev. B* **74**, 073414 (2006).
- ¹⁸ B. de Boer, A. Hadipour, M. M. Mandoc, T. van Woudenberg, and P. W. M. Blom, *Advanced Materials* **5**, 621 (2005).
- ¹⁹ L. Giordano, F. Cinquini, and G. Pacchioni, *Phys. Rev. B* **73**, 045414 (2006).
- ²⁰ L. Giordano, G. Pacchioni, J. Goniakowski, N. Nilius, E. D. L. Rienks, and H.-J. Freund, *Phys. Rev. Lett.* **101**, 026102 (2008).
- ²¹ R. M. Jacobs, J. H. Booske, and D. Morgan, *The Journal of Physical Chemistry C* **118**, 19742 (2014).
- ²² H. H. Arefi and G. Fagas, *The Journal of Physical Chemistry C* **118**, 14346 (2014).
- ²³ G. Giovannetti, P. A. Khomyakov, G. Brocks, V. M. Karpan, J. van den Brink, and P. J. Kelly, *Phys. Rev. Lett.* **101**, 026803 (2008).
- ²⁴ Y.-J. Yu, Y. Zhao, S. Ryu, L. E. Brus, K. S. Kim, and P. Kim, *Nano Letters* **9**, 3430 (2009).
- ²⁵ Suchitra, J. Pan, and U. V. Waghmare, *J. Appl. Phys.* **116**, 034304 (2014).
- ²⁶ V. S. Kumar and M. K. Niranjana, *Journal of Applied Physics* **115**, 173705 (2014).
- ²⁷ N. W. Ashcroft and N. D. Mermin, *Solid State Physics*, Holt, Rinehart and Winston (1976).
- ²⁸ H. B. Michaelson, *Journal of Applied Physics* **48**, 4729 (1977).
- ²⁹ H. Samata, Y. Saeki, S. Mizusaki, Y. Nagata, T. Ozawa, and A. Sato, *Journal of Crystal Growth* **311**, 623 (2009), the Proceedings of the 4th International Asian Conference on Crystal Growth and Crystal Technology.
- ³⁰ G. Kresse and D. Joubert, *Phys. Rev. B* **59**, 1758 (1999).
- ³¹ J. P. Perdew, K. Burke, and M. Ernzerhof, *Phys. Rev. Lett.* **77**, 3865 (1996).
- ³² J. P. Perdew and A. Zunger, *Phys. Rev. B* **23**, 5048 (1981).
- ³³ X. Fang and T. Kobayashi, *Applied Physics A* **69**, S587 (1999).
- ³⁴ T. Susaki, A. Makishima, and H. Hosono, *Phys. Rev. B* **84**, 115456 (2011).
- ³⁵ G. Koster, L. Klein, W. Siemons, G. Rijnders, J. S. Dodge, C.-B. Eom, D. H. A. Blank, and M. R. Beasley, *Rev. Mod. Phys.* **84**, 253 (2012).
- ³⁶ S. Ohta, T. Nomura, H. Ohta, and K. Koumoto, *Journal of Applied Physics* **97**, 034106 (2005).
- ³⁷ J. Heyd, G. E. Scuseria, and M. Ernzerhof, *The Journal of Chemical Physics* **118**, 8207 (2003).
- ³⁸ J. L. F. Da Silva, M. V. Ganduglia-Pirovano, J. Sauer, V. Bayer, and G. Kresse, *Phys. Rev. B* **75**, 045121 (2007).
- ³⁹ M. T. Greiner, L. Chai, M. G. Helander, W.-M. Tang, and Z.-H. Lu, *Advanced Functional Materials* **22**, 4557 (2012).
- ⁴⁰ S. L. Dudarev, G. A. Botton, S. Y. Savrasov, C. J. Humphreys, and A. P. Sutton, *Phys. Rev. B* **57**, 1505 (1998).
- ⁴¹ P. Hansmann, T. Ayril, L. Vaugier, P. Werner, and S. Biermann, *Phys. Rev. Lett.* **110**, 166401 (2013).
- ⁴² K. Yoshimatsu, K. Horiba, H. Kumigashira, T. Yoshida, A. Fujimori, and M. Oshima, *Science* **333**, 319 (2011).
- ⁴³ Z. Zhong, Q. Zhang, and K. Held, *Phys. Rev. B* **88**, 125401 (2013).
- ⁴⁴ M. Kawasaki, K. Takahashi, T. Maeda, R. Tsuchiya, M. Shinohara, O. Ishiyama, T. Yonezawa, M. Yoshimoto, and H. Koinuma, *Science* **266**, 1540 (1994).
- ⁴⁵ G. Koster, B. L. Kropman, G. J. H. M. Rijnders, D. H. A. Blank, and H. Rogalla, *Applied Physics Letters* **73**, 2920 (1998).
- ⁴⁶ N. Erdman, K. R. Poeppelmeier, M. Asta, O. Warschkow, D. E. Ellis, and L. D. Marks, *Nature* **419**, 55 (2002).
- ⁴⁷ R. Herger, P. R. Willmott, O. Bunk, C. M. Schlepütz, B. D. Patterson, and B. Delley, *Phys. Rev. Lett.* **98**, 076102 (2007).
- ⁴⁸ N. Nakagawa, H. Y. Hwang, and D. A. Muller, *Nature Materials* **5**, 204 (2006).
- ⁴⁹ T. Susaki, A. Makishima, and H. Hosono, *Phys. Rev. B* **83**, 115435 (2011).
- ⁵⁰ L. C. Allen, *Journal of the American Chemical Society* **111**, 9003 (1989).
- ⁵¹ S. Trasatti, *Journal of Electroanalytical Chemistry and Interfacial Electrochemistry* **33**, 351 (1971).
- ⁵² A. Radetinac, K. S. Takahashi, L. Alff, M. Kawasaki, and Y. Tokura, *Applied Physics Express* **3**, 073003 (2010).
- ⁵³ Z. Zhong, P. Wissgott, K. Held, and G. Sangiovanni, *Europhys. Lett.* **99**, 37011 (2012).
- ⁵⁴ For our qualitative discussion the specific type of the electronegativity (e.g. Pauling, Muliken, Allan, etc.) is not really important since materials trends are very similar for all schemes.
- ⁵⁵ Please note that SrTiO₃ as well as SrZrO₃ are band insulators such that we took the position of the lowest conduction

band as reference energy for the work function.